Published in final edited form as:
Int J Radiat Oncol Biol Phys. 2008 November 1; 72(3): 918–926. doi:10.1016/j.ijrobp.2008.06.1925.

Correlation between tumor growth delay and expression of cancer and host VEGF, VEGFR2 and osteopontin in response to radiotherapy

Timothy D. Solberg, Ph.D.[1,2], **Jessica Nearman, B.Sc.**[1], **John Mullins, B.Sc.**[1], **Sicong Li, D. Sc.**[1], and **Janina Baranowska-Kortylewicz, Ph.D.**[1*]

1*University of Nebraska Medical Center, Omaha, Nebraska*

2*University of Texas Southwestern Medical Center, Dallas, Texas*

Abstract

Purpose—to determine late effects of radiotherapy on the VEGF, VEGFR2 and OPN expression in cancer and stromal cells.

Methods and Materials—LS174T xenografted athymic mice were used as a tumor model. Radiation was delivered in two equivalent fractionation schemes: 5×7 Gy and 1×20 Gy, the latter at two dose rates.

Results—Tumor growth arrest was similar in all treatment groups with the exception of a better response of small-sized tumors in the 5×7 Gy group. Host VEGF and OPN levels were directly proportional to tumor doubling time (T_D) and were independent of the fractionation scheme. Host and cancer cell VEGFR2 levels in tumor were also directly related to the tumor response to radiotherapy.

Conclusion—Upregulated VEGFR2 in cancer cells suggest paracrine signaling in the VEGFR2 pathway of cancer cells as the factor contributing to the radiotherapy failure. The transient activation of the host VEGF/VEGFR2 pathway in tumor supports the model of angiogenic regeneration and suggests that radiation-induced upregulation of VEGF, VEGFR2, and downstream proteins may contribute to the failure of radiotherapy by escalating the rate of vascular repair. Co-expression of host OPN and VEGF, two factors closely associated with angiogenesis, indicate that OPN can serve as a surrogate marker of the tumor recovery after radiotherapy. Taken together these results strongly support the notion that to achieve optimal therapeutic outcome, the scheduling of radiation and anti-angiogenic therapies will require patient-specific post-treatment monitoring of the VEGF/VEGFR2 pathway and that tumor-associated OPN can serve as an indicator of the tumor regrowth.

Keywords

stereotactic body radiation therapy (SBRT); VEGF; VEGFR2; osteopontin

Corresponding author: Janina Baranowska-Kortylewicz, 986850 Nebraska Medical Center, Omaha, Nebraska 68198-6850, phone 402-559-8906, fax 402-559-9127, jbaranow@unmc.edu.

Meetings: presented in part at 49th Annual Meeting of ASTRO, 10/28/2007, Los Angeles.

Conflicts
None

Introduction

Interruption of the paracrine communication between tumor cells and tumor vasculature either through the blockade of vascular endothelial growth factor receptor-2 (VEGFR2) or through the neutralization of tumor-associated VEGF enhances antitumor activity of ionizing radiation[1–11]. Although this concept is not new, the optimal scheduling of these two modalities in relation to each other remains uncertain. Preclinical animal studies[1–3,5,6,10] as well as clinical trials[4,7,8–11] have called attention to the possibility that depending on the sequence of the applied treatments, anti-VEGFR2 and anti-VEGF therapies combined with ionizing radiation can be synergistic, additive, have no effect, and in some cases, can even compromise the outcome of radiotherapy[9,10].

Total radiation doses, dose per fraction, overall treatment time as well as the amount of anti-angiogenic therapy in combined treatments can impact the outcome[12]. However, timing and the sequence of therapeutic regimens are key factors, which ultimately dictate the outcome. For example, Williams *et al.*[13] used ZD6474, a potent VEGFR2 inhibitor, to augment radiation therapy of non-small-cell lung cancer in concurrent and sequential regimens. The tumor growth delay after the sequential schedule was significantly enhanced compared to the concurrent treatment. Impaired tumor reoxygenation between fractions in the concurrent protocol was suggested as the reason for these differences. Authors concluded that the clinical efficacy of ZD6474 as the adjuvant to radiation therapy will strongly depend on the course of therapy. In contrast, in a related study Brazell *et al.*[14] reported virtually identical tumor responses regardless of the treatment scheme.

Radiation alone can result in the intensification of the angiogenic processes[15] and contribute to the direct up-regulation of the VEGF expression in cancer cells[1]. This is a manifestation of the overall cellular response to stress associated with the induction of various genes, transcription factors and the activation of growth factors, and allied receptors. Tumor-associated host cells are attracted to cancer cells by VEGF and engage in a continuous exchange of molecular information with cancer cells, affecting tumor response to therapy, tumor invasion and metastasis. One of the outcomes of this complex communication is angiogenesis with VEGF as a dominant proangiogenic protein[16–18].

VEGF stimulates angiogenesis through cooperative mechanism involving VEGF-induced proteins in endothelial cells including osteopontin (OPN)[19]. OPN has diverse functions such as cell adhesion, chemoattraction, immunomodulation, and upregulation of the endothelial cell migration induced by VEGF. OPN expression is also correlated with tumor hypoxia[20]. Efforts of the past 25 years to develop VEGF-and VEGFR-targeted imaging probes are yet to produce clinically useful agents. Data suggest that surrogate markers are needed. Tumor-derived OPN shows positive correlation with VEGF and can trigger VEGF-dependent tumor progression and angiogenesis[19,20]. The reported here studies were designed to evaluate if similar positive correlation between OPN and VEGF exist in irradiated tumors and to establish the validity of OPN as a surrogate marker.

Of the three recognized receptors for the VEGF family of ligands, the activation of VEGFR2 (KDR, Flk-1) is sufficient to elicit all proangiogenic, proliferation and survival effects associated with VEGF[21–23]. The induction of VEGF by ionizing radiation is implicated in processes protecting tumor blood vessels and contributing to tumor radioresistance[1,12,24]. VEGF mRNA levels in irradiated Lewis lung carcinoma persisted at elevated levels two weeks after irradiation[1]. Anti-VEGF antibodies improved tumor response and this synergistic effect was attributed to the increased radiation-induced death of endothelial cells. Similar conclusions were derived from studies in glioblastoma cells, in which radiation-enhanced VEGF secretion was attributed to their increased radioresistance[12,24]. These and other preclinical studies have

shown that therapeutic benefits of radiation therapy may be greatly enhanced when used in combination with the inhibitors of the VEGFR2 pathway. Based on these findings several clinical protocols have been undertaken[7,8,11,25–26]. Early results are mixed. The emerging sense is that because the mechanism of the VEGF-VEGFR2 interactions with ionizing radiation is only partially defined, the design of some clinical studies may have been suboptimal[9,10]. A recent report on the effects of VEGF in several endothelial cell lines concluded that VEGF does not confer any significant level of radioprotection to these cells[27] suggesting that not all anti-VEGF therapies target tumor vasculature as it was previously hypothesized.

Here we demonstrate that irradiation of xenografts in athymic mice is associated with the induction of VEGF and VEGFR2. We also show that the expression of OPN, which cooperates with VEGF in proangiogenic processes, is significantly induced in response to ionizing radiation and in its expression parallels levels of the host VEGF in tumor suggesting OPN as an excellent alternative marker. This study reports for the first time the significant upregulation of the VEGFR2 expression by ionizing radiation in cancer cells and its direct relationship to the therapeutic response. Observations reported here also contribute the model of angiogenic regeneration[12,15,28], wherein the radiation-induced expression of VEGF, its allied receptor and the downstream proteins are a factor in the failure of radiotherapy by intensifying the vascular regrowth.

Methods and Materials

Animal and Tumor Models

Six-weeks old female mice (NCr-nu/nu) were from NCI. Subcutaneous tumors were produced after the injection of 5×10^6 LS174T human colorectal adenocarcinoma cells in 0.2 mL minimum essential medium (Invitrogen, Carlsbad, California). Cells were from sub-confluent monolayers grown in MEM supplemented with 10% fetal bovine serum.

Radiation Therapy (SBRT)

Mice were randomized as follows: no treatment (n = 12); RT of 5×7 Gy (n = 18), RT of 20 Gy at an instantaneous dose rate of 8 Gy/min (average 3 Gy/min; n = 15; 20-Gy-fast), and RT of 20 Gy at an instantaneous dose rate of 1.6 Gy/min (average 1.2 Gy/min; n =12, 20-Gy-slow). Irradiations lasted ~2–17 min, depending on the dose and dose rate.

Axial computed tomography was used to provide the depth and electron density information necessary for the treatment planning and dose computation. A custom bolus placed on xenografts provided adequate buildup for the high energy beam. Radiation was delivered through 15-mm or 17.5-mm circular collimators using x-rays produced by a 6-MV linear accelerator (Novalis, BrainLAB AG, Feldkirchen, Germany). The collimator size was selected to ensure complete coverage of tumor volume while producing a sharp radiation falloff for optimal sparing of normal anatomy. Three non-coplanar arcs spanning a total of 150° ensured uniform tumor coverage while minimizing peripheral dose.

Body weight and tumor sizes were measured three times per week; tumor volumes calculated using the formula for ellipsoid. Necropsy was performed 3 weeks after the first dose of SBRT. Gross evaluation of organs did not reveal any differences between groups. Hematocrit was determined by standard techniques. HemoCue® was used to measure hemoglobin levels (Ängelholm, Sweden). The remaining blood was used to prepare plasma, which was stored at −80°C until use. Tumors were frozen in liquid nitrogen and lysed as described below.

Preparation of Tumor Lysates

Frozen tumors were minced and transferred into a volume of ice-cold lysis buffer equivalent to two tumor weights (20 mM Tris, pH 7.5, 150 mM NaCl, 1 mM EDTA, 1 mM EGTA, 1% Triton X-100, 2.5 mM $Na_4O_7P_2$, 1 mM β-glycerol-phosphate, 1 mM Na_3VO_4, 1μg/mL leupeptin, supplemented with 1 mM PMSF). Minced tumor fragments were sonicated on ice using a Vibra Cell Model VC 375 ultrasonic processor (Sonics&Materials, Inc., Danbury, CT, USA) for 14 s with a 14-s break between sonications; total of 4 min at a 40% duty cycle. Homogenates were centrifuged at 14,000×*g* for 10 min at 4°C. Supernatants were aliquoted and stored at −80°C after the total protein content was determined using the micro-BCA assay (Pierce Biotechnology, Rockford, IL).

Determination of Human and Mouse VEGF

Quantikine mouse VEGF (mVEGF) and human VEGF (hVEGF) quantitative sandwich enzyme immunoassays from R&D Systems, Inc. (Minneapolis, MN) were used according to the manufacturer's instructions. To measure mVEGF, aliquots of tumor lysates containing 0.08 mg total protein were diluted with RD1N and added to wells. Plasma was diluted at 1:1 (v/v) ratio with RD5T before adding to wells. Analyses of hVEGF required 0.01 mg total protein diluted with RD1W. Plasma was diluted also at 1:1 ratio with RD6U before adding to wells.

Mouse and Human Osteopontin

TiterZyme® kits were from Assay Designs (Ann Arbor, Michigan) and were used as directed by the vendor. Recombinant mOPN was used as a standard. ~Four % crossreactivity with human OPN is observed. Recombinant hOPN was used to prepare the standard curve for human OPN determination. There is no crossreactivity with mOPN.

Determination of mouse and human VEGFR2

Tumor lysates were prepared as described above. Protein samples were resolved on 4–20% gradient minigels (BioRad, Hercules, CA) and transferred overnight onto Hybond™-P 0.45-μm PVDF membranes (Amersham Biosciences, Piscataway, NJ) at 14 mV for 18 h at 4°C. Membranes were incubated in 5% BSA, 10 mM Tris-HCl, pH 7.5, 100 mM NaCl, 0.1% Tween-20 overnight at 4°C to reduce nonspecific binding. Blocked membranes were incubated overnight at 4°C in the same buffer containing anti-human VEGFR2 antibody MAB3571 (R&D Systems, Minneapolis, MN) at 1:5,000 dilution followed by HRP-linked goat anti-mouse IgG secondary antibody 31430 at a 1:150,000 dilution for 1 h at rt (Pierce Biotechnology). Antigens were detected using ChemiGlow® according to the manufacturer instructions (Alpha Innotech Corporation, San Leandro, CA). Membranes were stripped and re-probed with rabbit anti-β-actin 13E5 (Cell Signaling Technology, Danvers, MA) at 1:5,000 dilution. Protein band intensity was measured using ImageJ (http://rsb.info.nih.gov/ij/) and normalized to the β-actin band intensity as the internal standard. Several anti-mouse VEGFR2 antibodies were also evaluated; all gave unacceptable levels of nonspecific binding. For this reason the definite determination of mouse VEGFR2 was done using the ELISA assay (R&D Systems, Minneapolis, MN).

Statistical Analyses

Tumor size and body weight changes were normalized to values on the day of the first SBRT treatment and are expressed as either mean±std dev or mean±sem. Summary statistics were performed using a two-sided, unpaired Student's t-test with a significance level of P=0.05. Tumor doubling times (T_D) were calculated from data of all mice in each group using the curve fitting function of SigmaPlot/SigmaStat (Systat Software, Inc. Point Richmond, CA). Kaplan-Meier survival analyses were done using MedCalc Software (Mariakerke, Belgium). The Mann-Whitney rank sum test for tumor T_D analyses was done using the SigmaPlot/SigmaStat.

Results

Radiotherapy

Radiation dose was prescribed at the 90% isodose volume, which completely encompassed the xenograft (Fig.1). The use of clinical radiosurgery equipment in pre-clinical irradiation has been described previously[29,30]. Dose equivalence was calculated from the linear-quadratic model using a tumor α/β ratio of 10. Dose/fraction schemes were selected based on their relevance to clinical practice of SBRT.

General health

Hemoglobin (Hb) and hematocrit (Hct) were measured for each mouse during the necropsy. Both parameters were within the normal range. Body weight changes after treatment reflected the overall health of mice and were essentially parallel to changes in blood parameters. In the 5×7 Gy and 20-Gy-fast groups, mice with small tumors fared better compared to mice with the initially larger sized tumors (Fig.2). However, these differences are not statistically significant. On the whole mice were healthy, although some lost ~10–15% of their body weight over a period of one week after treatment. This weight loss remained at the plateau for ~5–7 days and was followed by the gradual weight gains.

Tumor growth rates

Radiation doses delivered in five fractions produced significantly better response in tumors that were <0.4 g on the day of the first radiation dose compared to tumors that were >0.4 g on the same day. Tumor growth curves (Fig.3A) and the necropsy data coincide (Fig.3B–D). The 20-Gy-fast dosing scheme initially produced in small tumors good responses lasting ~10 days, after which time the exponential growth resumed. Unlike small tumors in the 5×7 Gy group, which produced far better responses compared to large tumors (Fig.4), small tumors in both 20 Gy groups responded at approximately the same rate as large tumors. T_Ds (Table 1) as well as necropsy data confirm this result (Fig.3B,C,D). However, when at each dose level all necropsied tumors are analyzed collectively, the differences between groups become less apparent (Fig.3B). It is evident that any difference in tumor response to various dosing schemes is derived from the superior responses of smaller tumors (Fig.3C). Tumor weights at necropsy in groups with large initial tumors were 1.33±0.34 g, 1.62±0.44 g, and 1.49±0.89 g in 5×7 Gy, 20-Gy-fast, and 20-Gy-slow groups, respectively, and are not statistically different (Fig.3D). Respective T_Ds for these tumors in all treatment groups were ~15 days (Table 1). Tumor weights in groups with the initially smaller tumors ranged from 0.49±0.21 g for the 5×7 Gy-treated mice, to 0.79±0.24 g and 1.12±0.56 g for the 20-Gy-fast and 20-Gy-slow treated mice, respectively (Fig.3C). T_Ds calculated from the tumor growth curves also followed this trend, with T_D=21±1.4 days in the 5×7 Gy group, and ~12 days in both 20 Gy groups. Average T_D in the group of untreated control mice was ~3.6 days. Kaplan-Meier analyses using the probability of tumor doubling as the end point yielded results similar to monoexponential analyses of growth curves, and confirmed that tumors <0.4 g the initial size were the best responders when treated with 5×7 Gy (Table 2 and Fig.4).

Expression of VEGF and OPN

Levels of VEGF of the human and mouse origin were measured in plasma and tumors obtained during necropsy. Lysates were prepared either from individual tumors or from combined samples of tumors exhibiting similar growth characteristics. The expression of mVEGF in tumor is directly proportional to T_D, i.e., the longer T_D (slower tumor growth), the higher the levels of mVEGF at necropsy. A comparable relationship is absent for hVEGF (Fig.5A). The strong relationship between the mVEGF expression in selected xenografts and their individual growth curves in several mice is illustrated in Fig.5B.

In plasma, hVEGF was undetectable. Circulating levels of mVEGF were high and practically identical in all mice independent of the radiation dose, T_D and the tumor size. The average mVEGF in plasma was measured at 1,039±96 pg/mL.

High levels of mOPN were detected in irradiated xenografts. The expression of mOPN is directly proportional to levels of mVEGF in tumor (Fig.5C) indicating that tumor-associated mOPN can serve as the alternative indicator of the onset of the VEGF-stimulated angiogenesis, which typically proceeds via a cooperative mechanism involving VEGF-induced proteins in endothelial cells including OPN[19]. In contrast, hOPN is not present in LS174T xenografts.

Expression of VEGFR2 in tumor

Western blot analyses of hVEGFR2 are shown in Fig.6A. It is evident that hVEGFR2 levels are dependent on the tumor response and that these levels are directly proportional to T_D (Fig. 7A). Host mVEGFR2 is elevated in all tumors (Fig.6B) compared to untreated controls. The exception were tumors in the 20-Gy-fast group with the initial size of >0.4 g (Fig.7B). However, no clear association between mVEGFR2 and the individual tumor response is apparent. Similarly, when levels of mVEGFR2 are analyzed relative to the expression of mVEGR2 in untreated tumors, only in the 20-Gy-fast mVEGFR2 remains unchanged compared to controls whereas all other groups have significantly elevated levels of mVEGFR2 (Fig.7B).

Discussion

While the pretreatment status of VEGF and VEGFR2 is considered predictive of the tumor response to various forms of therapy[31–35], the post-treatment evaluation of VEGF and VEGFR2 expression does not seem to play any part in the follow up. The activation of the VEGF/VEGFR2 pathway reported in these studies suggests that post-treatment longitudinal evaluations of tumor-associated VEGF and VEGFR2 can provide significant insights into the tumor response and can aid in planning of the follow up treatment. Moreover, the strong link observed between host OPN and host VEGF in tumors indicates that in the absence of suitable noninvasive methods to measure tumor-associated VEGF, OPN can serve as an excellent surrogate marker.

VEGFR2 mediates the majority of the downstream effects of VEGF in angiogenesis. The observed here upregulation of tumor-associated hVEGFR2 and increased levels of mVEGF indicate the paracrine activation of the tumor cell's VEGF/VEGFR2 pathway. The direct proportionality of T_D and levels of host VEGF (Fig.5A) and elevated expression of host VEGFR2 (Fig.6B,7B) are indicative of the process of the angiogenic regeneration. Results presented here shed light on a unique aspect of the tumor regrowth and its relationship to angiogenic activities in the host and cancer cells, and contribute further empirical support to the angiogenic regeneration hypothesis[15]. In the tumors that responded better to radiation, increased VEGFR2/VEGF levels appeared to correlate with delayed tumor regrowth (i.e., longer TD); however, in poor responders, with a shorter TD, the activation of VEGF/VEGFR2 was not apparent at necropsy, i.e., it probably occurred earlier in the post-treatment period, and, at necropsy, it had already reached the untreated control levels (Fig.5B›Fig.6A›Fig.7A). This relationship is also evident in the expression of tumor-associated mouse OPN, an observation similar to the reported pre-treatment osteopontin expression in prostate cancer[36]. Apparently, pre-treatment OPN is not a predictor of a shorter time to biochemical failure in prostate cancer, whereas increased post-treatment levels of OPN are significantly associated with a shorter time to biochemical failure[36].

Endothelial cells in tumor vasculature exhibit the upregulated VEGFR2 expression. Typically, VEGFR2 is 3-5-fold higher in tumor vasculature compared to normal vasculature[37,38]. VEGF stimulates *VEGFR*2 gene expression in endothelial cells via a positive feedback

mechanism[39]. Reports indicate that whereas tumor cells have high levels of VEGF, only rarely is a notable VEGFR2 expression observed[40,41]. The role of tumor-secreted VEGF in the pathological angiogenesis via stimulation of VEGFR2 expressed on tumor endothelial cells is well established and suggest a paracrine loop between tumor cells and vascular endothelial cells[39,42]. However, the role of VEGFR2 expressed by tumor cells is not fully understood, although emerging evidence suggests that host VEGF plays a role in the cancer development through VEGFR2 on tumors cells.

Studies described here demonstrate for the first time a strong and concomitant activation of VEGFR2 in cancer cells and VEGF and OPN in host cells in response to radiation therapy suggesting a dual role for the upregulated host VEGF and cooperative interaction with OPN. Tumor-derived OPN contributes to tumor progression and recurrence via VEGF-dependent angiogenesis[19,20,43]. The paracrine signaling from the host VEGF to cancer cell VEGFR2 may be a significant component of radiation therapy failures. Furthermore, these results indicate that monitoring of the post-treatment activation of VEGF/VEGFR2 pathway, either directly or via OPN, may be important in assessing clinical response to multimodality radiotherapy regimens. In conclusion, to achieve optimal therapeutic outcome, the scheduling of radiation and anti-angiogenic therapies will require patient-specific noninvasive monitoring of the post-treatment changes in the VEGF/VEGFR2 pathway.

Acknowledgments

Financial support provided by R01CA95267 (JBK), Department of Radiation Oncology, and American Cancer Society grant 03-028-01-CCE (TDS).

Bibliography

1. Gorski DH, Beckett MA, Jaskowiak NT, et al. Blockage of the vascular endothelial growth factor stress response increases the antitumor effects of ionizing radiation. Cancer Res 1999;59:3374–3378. [PubMed: 10416597]
2. Kozin SV, Boucher Y, Hicklin DJ, et al. Vascular endothelial growth factor receptor-2-blocking antibody potentiates radiation-induced long-term control of human tumor xenografts. Cancer Res 2001;61:39–44. [PubMed: 11196192]
3. Winkler F, Kozin SV, Tong RT, et al. Kinetics of vascular normalization by VEGFR2 blockade governs brain tumor response to radiation: role of oxygenation, angiopoietin-1, and matrix metalloproteinases. Cancer Cell 2004;6:553–563. [PubMed: 15607960]
4. Willett CG, Boucher Y, di Tomaso E, et al. Direct evidence that the VEGF-specific antibody bevacizumab has antivascular effects in human rectal cancer. Nat Med 2004;10:145–147. [PubMed: 14745444]
5. Zips D, Hessel F, Krause M, et al. Impact of adjuvant inhibition of vascular endothelial growth factor receptor tyrosine kinases on tumor growth delay and local tumor control after fractionated irradiation in human squamous cell carcinomas in nude mice. Int J Radiat Oncol Biol Phys 2005;61:908–914. [PubMed: 15708274]
6. Wachsberger PR, Burd R, Marero N, et al. Effect of the tumor vascular-damaging agent, ZD6126, on the radioresponse of U87 glioblastoma. Clin Cancer Res 2005;11:835–842. [PubMed: 15701874]
7. Maurel J, Martin-Richard M, Conill C, et al. Phase I trial of gefitinib with concurrent radiotherapy and fixed 2-h gemcitabine infusion, in locally advanced pancreatic cancer. Int J Radiat Oncol Biol Phys 2006;66:1391–1398. [PubMed: 16965868]
8. Willett CG, Duda DG, diTomaso E, et al. Complete pathological response to bevacizumab and chemoradiation in advanced rectal cancer. Nat Clin Pract Oncol 2007;4:316–321. [PubMed: 17464339]
9. Senan S, Smit EF. Design of clinical trials of radiation combined with antiangiogenic therapy. Oncologist 2007;12:465–477. [PubMed: 17470689]

10. Horsman MR, Siemann DW. Pathophysiologic effects of vascular-targeting agents and the implications for combination with conventional therapies. Cancer Res 2006;66:11520–11539. [PubMed: 17178843]
11. Czito BG, Bendell JC, Willett CG, et al. Bevacizumab, oxaliplatin, and capecitabine with radiation therapy in rectal cancer: Phase I trial results. Int J Radiat Oncol Biol Phys 2007;68:472–478. [PubMed: 17498568]
12. Gupta VK, Jaskowiak NT, Beckett MA, et al. R. Vascular endothelial growth factor enhances endothelial cell survival and tumor radioresistance. Cancer J 2002;8:47–54. [PubMed: 11895203]
13. Williams KJ, Telfer BA, Brave S, et al. ZD6474, a potent inhibitor of vascular endothelial growth factor signaling, combined with radiotherapy: schedule-dependent enhancement of antitumor activity. Clin Cancer Res 2004;10:8587–8593. [PubMed: 15623642]
14. Brazelle WD, Shi W, Siemann DW. VEGF-associated tyrosine kinase inhibition increases the tumor response to single and fractionated dose radiotherapy. Int J Radiat Oncol Biol Phys 2006;65:836–841. [PubMed: 16751064]
15. Koukourakis MI, Giatromanolaki A, Sivridis E, et al. Squamous cell head and neck cancer: evidence of angiogenic regeneration during radiotherapy. Anticancer Res 2001;21:4301–4309. [PubMed: 11908684]
16. Folkman J. Angiogenesis in cancer, vascular, rheumatoid and other disease. Nat Med 1995;1:27–31. [PubMed: 7584949]
17. Bergers G, Benjamin LE. Tumorigenesis and the angiogenic switch. Nat Rev Cancer 2003;3:401–410. [PubMed: 12778130]
18. Ferrara N, Gerber HP, LeCouter J. The biology of VEGF and its receptors. Nat Med 2003;9:669–676. [PubMed: 12778165]
19. Senger DR, Ledbetter SR, Claffey KP, et al. Stimulation of endothelial cell migration by vascular permeability factor/vascular endothelial growth factor through cooperative mechanisms involving the alphavbeta3 integrin, osteopontin, and thrombin. Am J Pathol 1996;149:293–305. [PubMed: 8686754]
20. Hill RP. Targeted treatment: Insights from studies of osteopontin and hypoxia. Lancet Oncol 2005;6:733–734. [PubMed: 16198974]
21. Witte L, Hicklin DJ, Zhu Z, et al. Monoclonal antibodies targeting the VEGF receptor-2 (Flk1/KDR) as an anti-angiogenic therapeutic strategy. Cancer Metastasis Rev 1998;17:155–161. [PubMed: 9770111]
22. McMahon G. VEGF receptor signaling in tumor angiogenesis. The Oncologist 2000;5:3–10. [PubMed: 10804084]
23. Gille H, Kowalski J, Li B, et al. Analysis of biological effects and signaling properties of Flt-1 (VEGFR-1) and KDR (VEGFR-2). J Biol Chem 2001;276:3222–3230. [PubMed: 11058584]
24. Hovinga KE, Stalpers LJ, van Bree C, et al. Radiation-enhanced vascular endothelial growth factor (VEGF) secretion in glioblastoma multiforme cell lines-a clue to radioresistance? J Neurooncol 2005;74:99–103. [PubMed: 16193379]
25. Stopeck A, Sheldon M, Vahedian M, et al. Results of a Phase I dose-escalating study of the antiangiogenic agent, SU5416, in patients with advanced malignancies. Clin Cancer Res 2002;8:2798–2805. [PubMed: 12231519]
26. Bonner JA, Giralt J, Harari PM, et al. Cetuximab prolongs survival in patients with locoregionally advanced squamous cell carcinoma of head and neck: A phase III study of high dose radiation therapy with or without cetuximab. Proc Am Soc Clin Oncol 2004;22:5507.
27. Donker M, Van Furth WR, Mulder-Van Der Kracht S, et al. Negligible radiation protection of endothelial cells by vascular endothelial growth factor. Oncol Rep 2007;18:709–714. [PubMed: 17671724]
28. Heissig B, Rafii S, Akiyama H, et al. Low-dose irradiation promotes tissue revascularization through VEGF release from mast cells and MMP-9-mediated progenitor cell mobilization. J Exp Med 2005;202:739–750. [PubMed: 16157686]
29. Solberg TD, DeSalles AAF, Hovda D, et al. A Universal, Multi-Modality Localization System for animal radiosurgery. Acta Neurochirurgica 1994;62:28–32. [PubMed: 7717131]

30. Sun B, DeSalles AAF, Medin P, et al. Reduction of hippocampal-kindled seizure activity in rats by stereotactic radiosurgery. Exp Neurology 1998;154:691–695.

31. Lee JC, Chow NH, Wang ST, et al. Prognostic value of vascular endothelial growth factor expression in colorectal cancer patients. Eur J Cancer 2000;36:748–753. [PubMed: 10762747]

32. Takahashi Y, Kitadai Y, Bucana CD, et al. Expression of vascular endothelial growth factor and its receptor, KDR, correlates with vascularity, metastasis, and proliferation of human colon cancer. Cancer Res 1995;55:3964–3968. [PubMed: 7664263]

33. Manders P, Beex LV, Tjan-Heijnen VC, et al. The prognostic value of vascular endothelial growth factor in 574 node-negative breast cancer patients who did not receive adjuvant systemic therapy. Br J Cancer 2002;87:772–778. [PubMed: 12232762]

34. Fontanini G, Lucchi M, Vignati S, et al. Angiogenesis as a prognostic indicator of survival in non-small-cell lung carcinoma: A prospective study. J Natl Cancer Inst 1997;89:881–886. [PubMed: 9196255]

35. Gorski DH, Leal AD, Goydos JS. Differential expression of vascular endothelial growth factor-A isoforms at different stages of melanoma progression. J Am Coll Surg 2003;197:408–418. [PubMed: 12946796]

36. Vergis R, Corbishley CM, Norman AR, et al. Intrinsic markers of tumour hypoxia and angiogenesis in localised prostate cancer and outcome of radical treatment: a retrospective analysis of two randomised radiotherapy trials and one surgical cohort study. Lancet Oncol 2008;9:342–351. [PubMed: 18343725]

37. Plate KH, Breier G, Weich HA, et al. Vascular endothelial growth factor and glioma angiogenesis: coordinate induction of VEGF receptors, distribution of VEGF protein and possible in vivo regulatory mechanisms. Int J Cancer 1994;59:520–529. [PubMed: 7525492]

38. Neuchrist C, Erovic BM, Handisurya A, et al. Vascular endothelial growth factor receptor 2 (VEGFR2) expression in squamous cell carcinomas of the head and neck. Laryngoscope 2001;111:1834–1841. [PubMed: 11801954]

39. Ferrara N, Davis-Smyth T. The biology of vascular endothelial growth factor. Endocr Rev 1997;18:4–25. [PubMed: 9034784]

40. Dias S, Hattori K, Heissig B, et al. Inhibition of both paracrine and autocrine VEGF/VEGFR-2 signaling pathways is essential to induce long term remission of xenotransplanted human leukemias. Proc Natl Acad Sci U S A 2001;98:10857–10862. [PubMed: 11553814]

41. Ferrer FA, Miller LJ, Lindquist R, et al. Expression of vascular endothelial growth factor receptors in human prostate cancer. Urology 1999;54:567–572. [PubMed: 10475375]

42. Alitalo K, Carmeliet P. Molecular mechanisms of lymphangiogenesis in health and disease. Cancer Cell 2002;1:219–227. [PubMed: 12086857]

43. Shijubo N, Uede T, Kon S, et al. Vascular endothelial growth factor and osteopontin in stage I lung adenocarcinoma. Am J Respir Crit Care Med 1999;160:1269–1273. [PubMed: 10508818]

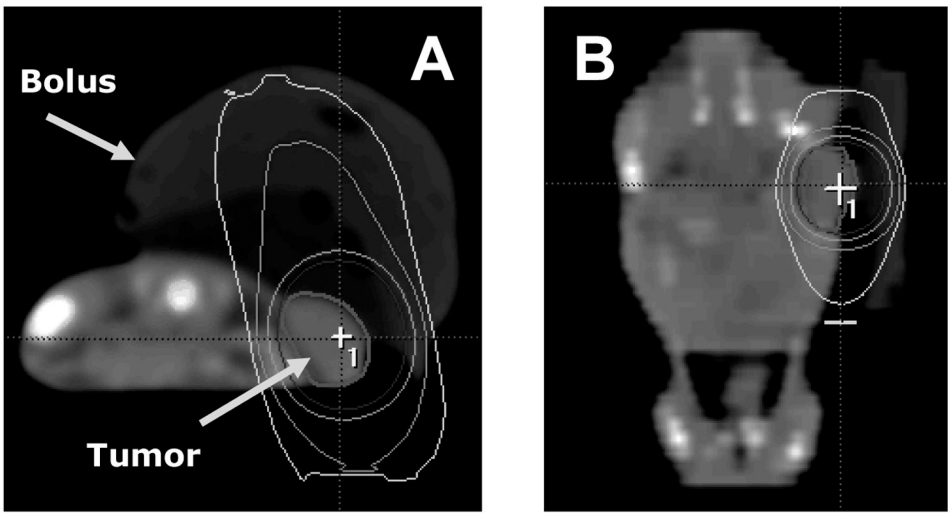

Fig. 1.
Axial CT scan with tumor and bolus indicated (A). Tumor is within the 90% isodose line. Note the sharp dose fall-off medially and sparing of all non-tumor anatomy in the coronal reconstruction (B).

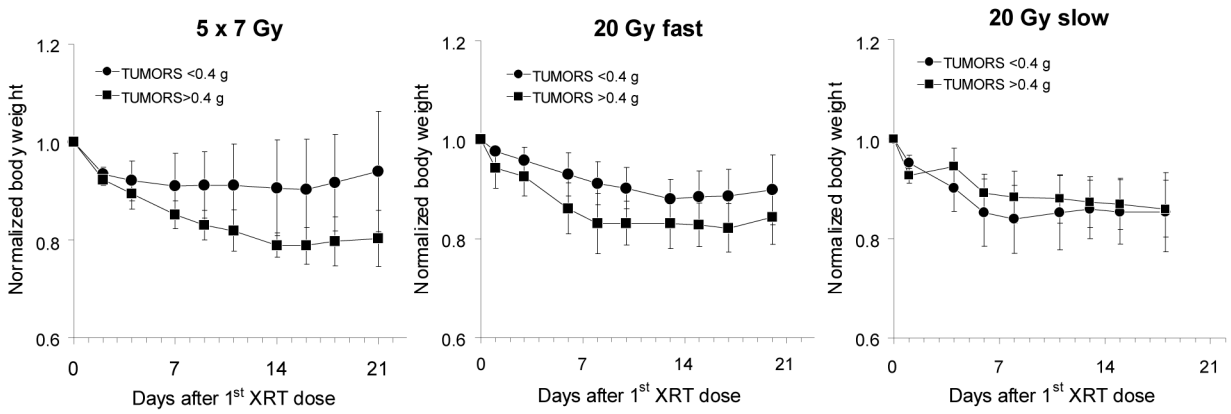

Fig. 2.

Body weight changes after radiotherapy (mean±std dev). Values are corrected for tumor size and normalized to weights on the day of the first treatment.

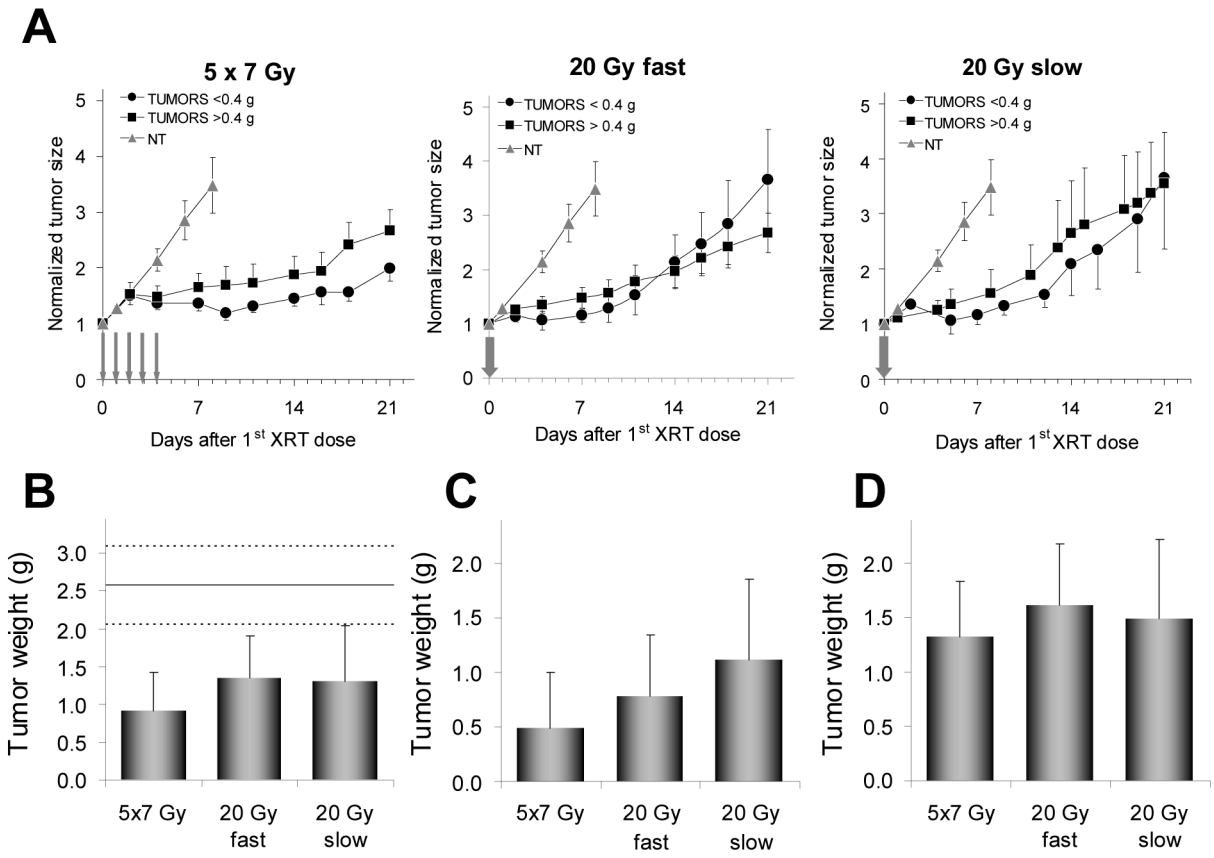

Fig. 3.

A. Tumor growth curves of LS174T xenografts implanted subcutaneously in athymic mice after radiotherapy. Values (mean±sem) are normalized to tumor volume on the day of the first treatment. **B**. Average tumor weights for all subjects in a given treatment group determined during necropsy. Solid line represents average tumor weights in untreated mice. Dotted lines are ±sem. **C**. Average tumor weights in mice with the initial tumor size of <0.4 g. **D**. Average tumor weights with the initial tumor size of >0.4 g (mean±sem).

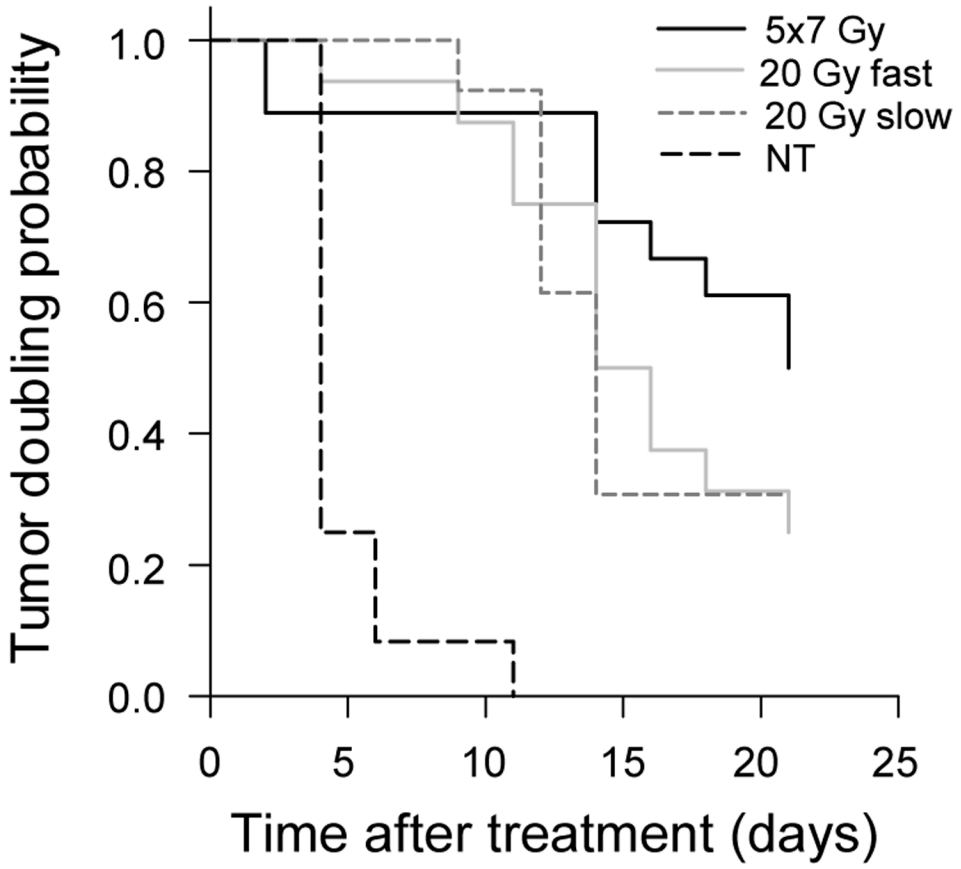

Fig. 4.
Kaplan-Meier analyses of tumor doubling times.

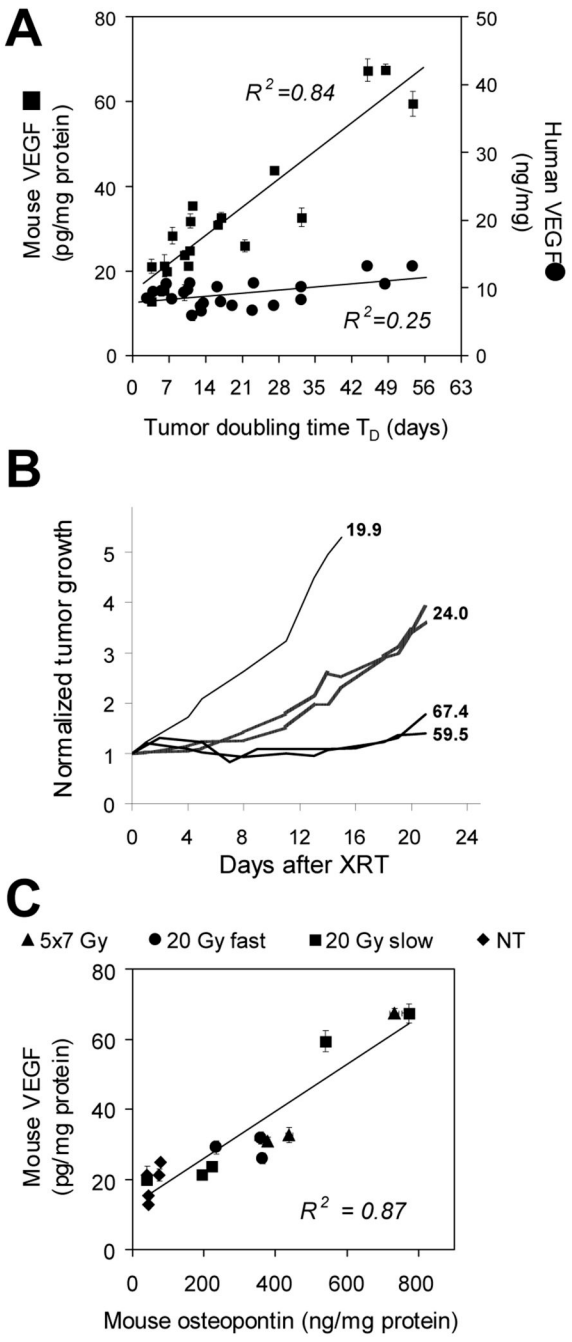

Fig. 5.

Expression of VEGF and OPN in LS174T tumors collected at necropsy 21 days after treatment. **A**. Relationship between T_D and host (■) and tumor (●) VEGF. Mouse VEGF levels are directly proportional to T_D. **B**. Examples of normalized growth curves for individual LS174T xenografts either irradiated with 20 Gy dose at 1.2 Gy/min (thick lines) or left untreated (thin line). Several examples are shown to better illustrate strong relationship between mVEGF and tumor response. Numbers to the right of each line represent pg mVEGF/mg total protein in tumor lysates. **C**. Correlation between host OPN and host VEGF levels in tumor.

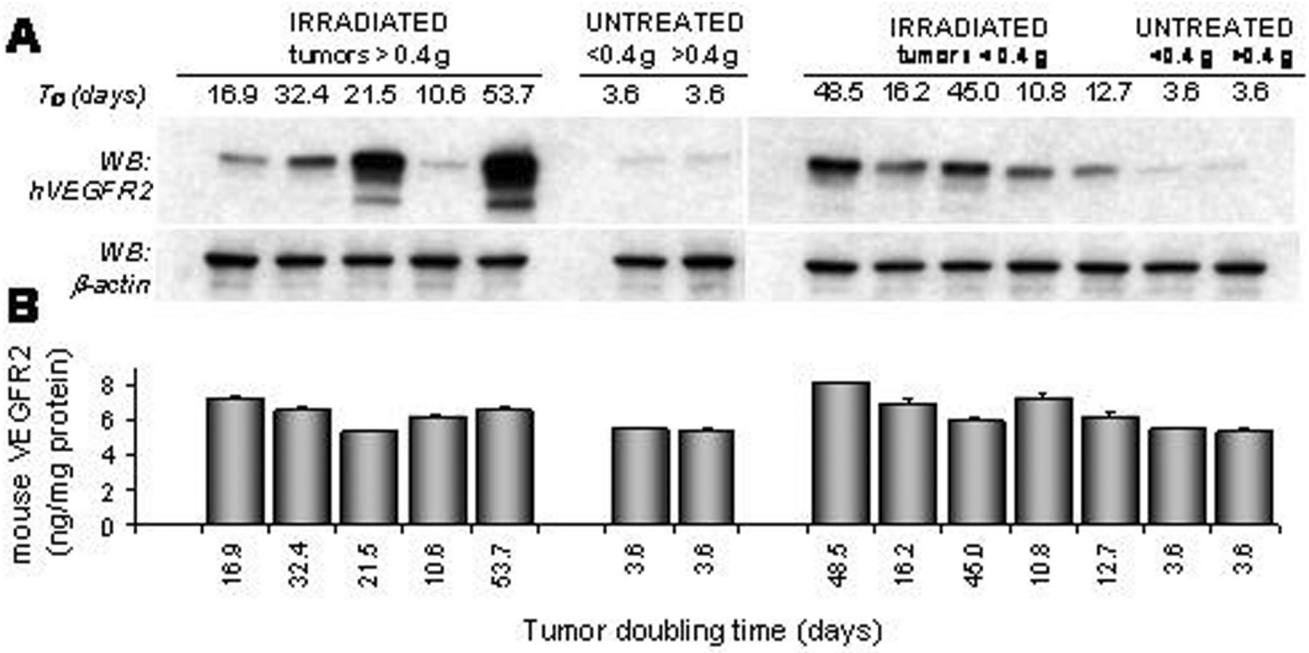

Fig. 6.

Expression of human and mouse VEGFR2 in LS174T xenografts 21 days after the first radiation dose. Untreated control mice (NT) were killed on day 15. **A**. Western immunoblot analyses of tumor lysates probed for human VEGFR2. β-Actin is the internal marker of the protein load. **B**. ELISA analyses of mouse VEGFR2 in the same lysates.

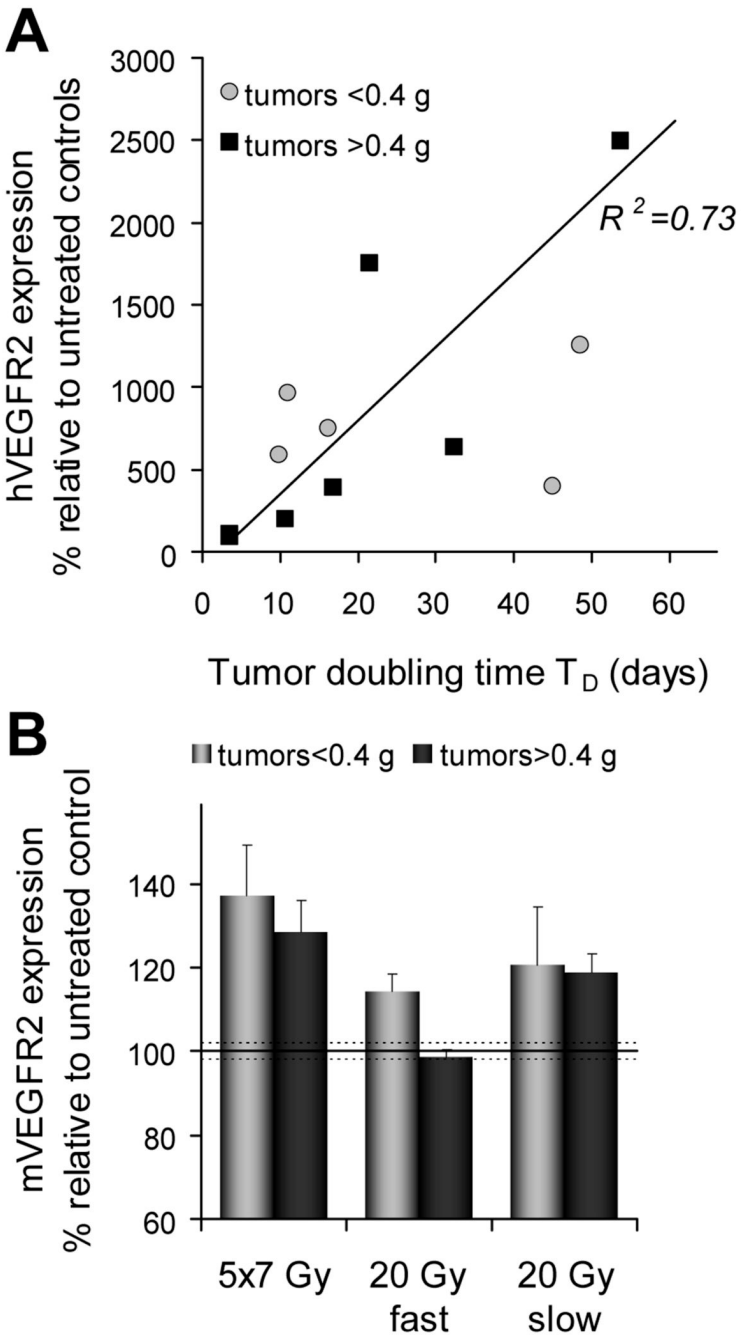

Fig. 7.
Human (**A**) and mouse (**B**) VEGFR2 levels in LS174T tumors expressed as the percent change relative to untreated control xenografts.

Table 1

Tumor doubling times derived from a single parameter, monoexponential tumor growth equation $y = e^{(\alpha t)}$

TUMORS <0.4 g	T_D (days)	sem (days)	R^2	Mann-Whitney rank sum test*
5×7 Gy	21.0	1.4	0.92	***0.033***
20 Gy fast	12.8	0.9	0.79	0.847
20 Gy slow	12.0	0.6	0.90	0.063
TUMORS >0.4 g				
5×7 Gy	14.6	1.0	0.83	
20 Gy fast	14.5	0.6	0.92	
20 Gy slow	14.8	0.8	0.91	
NT controls	3.6	0.2	0.87	

*P values comparing growth curves of tumors <0.4 g and tumors >0.4 g.

Table 2

Kaplan-Meier analyses of the tumor doubling probability analyzed using the Gehan-Breslow test for the survival curves with pair-wise multiple comparison procedures using the Holm-Sidak method.

TUMORS <0.4 g	**T_D (days)**	**sem (days)**
5×7 Gy	19.7	1.0
20 Gy fast	14.5	0.5
20 Gy slow	13.3	1.9
TUMORS >0.4 g		
5×7 Gy	14.9	2.8
20 Gy fast	15.3	1.6
20 Gy slow	16.7	1.7
NT controls	4.9	0.6